Title

Successful correction of factor V deficiency of patient-derived iPSCs by CRISPR/Cas9-mediated gene editing

Running head

Therapeutic genome editing for factor V deficiency

Authors

Takayuki Nakamura[1], Satoshi Morishige[1], Hidetoshi Ozawa[1], Kenji Kuboyama[2], Yoshitaka Yamasaki[1], Shuki Oya[1], Maki Yamaguchi[1], Kazutoshi Aoyama[1], Ritsuko Seki[1], Fumihiko Mouri[1], Koichi Osaki[1], Takashi Okamura[1,3], Shinichi Mizuno[1,4], and Koji Nagafuji[1]*

Affiliations

[1]Division of Hematology and Oncology, Department of Medicine, Kurume University School of Medicine, 67 Asahi-machi, Kurume 830-0011, Japan

[2]Department of Clinical Laboratory Medicine, Kurume University Hospital, 67 Asahi-machi, Kurume 830-0011, Japan

[3]Center for Hematology and Oncology, St. Mary's Hospital, 422 Tsubuku-Honmachi, Kurume 830-8543, Japan

[4]Division of Medical Sciences and Technology, Department of Health Sciences, Faculty of Medical Sciences, Kyushu University, 3-1-1 Maidashi, Higashi-Ku, Fukuoka 812-8582, Japan

Corresponding author:

*Koji Nagafuji, MD, PhD

Division of Hematology and Oncology, Department of Medicine, Kurume University School of Medicine, 67 Asahi-machi, Kurume 830-0011, Japan

E-mail: knagafuji@med.kurume-u.ac.jp

Tel: +81-942-31-7852

Fax: +81-942-31-7854

Word Count; 2914

Abstract

Background: Factor V (FV) deficiency is a monogenic inherited coagulation disorder considered to be an ideal indication for gene therapy. To investigate the possibility of therapeutic application of genome editing, we generated induced pluripotent stem cells (iPSCs) from a FV-deficient patient and repaired the mutation of factor V gene (*F5*) using a clustered regularly interspaced short palindromic repeats (CRISPR)/CRISPR-associated 9 (Cas9).

Methods: The patient's peripheral blood mononuclear cells were reprogrammed for iPSCs. The targeting vector was designed with homology arms against *F5* containing the corrected sequence. Cas9 ribonucleoprotein (RNP) complex and targeting vector were electroporated into iPSCs. Gene-edited iPSCs were differentiated into hepatocyte-like cells (HLCs).

Results: The mutation of *F5* in patient-derived iPSCs was repaired by CRISPR/Cas9. In concentrated culture supernatants of patient-derived iPS-HLCs, neither FV antigen nor activity were detected, while in those of gene-corrected iPS-HLCs, FV antigen and specific activity were 67.0 ± 13.1 ng/ml and 173.2 ± 41.1 U/mg, respectively.

Conclusions: We successfully repaired the mutation of *F5* using the CRISPR/Cas9 and confirmed the recovery of FV activity with gene-corrected iPS-HLCs. Gene-edited iPSCs will hold promise for gene therapy of inherited coagulation disorders as a potential cell source for autologous cell transplantation.

Keywords: clustered regularly interspaced short palindromic repeats, CRISPR-associated proteins, factor V deficiency, gene editing, induced pluripotent stem cells

Introduction

Coagulation factor V (FV) deficiency, also known as parahaemophilia, is a rare bleeding disorder, with frequency is estimated as one case per million people. FV deficiency can be classified as (1) type I deficiency, or cross-reacting material negative (CRM–) defect, with concordantly low or unmeasurable antigen and functional level (quantitative defect); (2) type II deficiency, or CRM+ defect, with normal or mildly reduced antigen level associated with reduced coagulant activity (qualitative defect) [1]. FV deficiency is usually asymptomatic, whereas some patients with a low FV coagulant activity level may exhibit severe bleeding manifestations including nasal, muscle, intracranial, or gastrointestinal hemorrhages. FV deficiency is inherited as an autosomal recessive trait and caused by genetic variants on the factor V gene (*F5*) located on chromosome 1q23. Here, we repaired the mutation of *F5* using a clustered regularly interspaced short palindromic repeats (CRISPR)/CRISPR-associated 9 (Cas9) system [2-4].

We demonstrated genome editing using induced pluripotent stem cells (iPSCs) derived from a patient's peripheral blood mononuclear cells (PBMCs), and differentiated gene-

corrected iPSCs into hepatocyte-like cells (HLCs) *in vitro* and measured the levels of FV antigen and activity in their culture supernatants.

Materials and Methods

Patient

A 55-year-old woman who is an offspring of consanguineous marriage and was diagnosed with ovarian cancer was the subject of this study. Routine coagulation tests before surgery revealed prolonged prothrombin time (PT) and activated partial thromboplastin time (APTT). A blood test showed that FV clotting activity was less than 3% (normal range: 70–135%) and FV antigen was less than 2% (normal average: 60-150%) [5]. The study protocol was reviewed and approved by the institutional review board of the Ethics Committee of the Kurume University School of Medicine, and the patient signed an informed consent form in accordance with the Helsinki Declaration.

Cell culture

All cells were maintained at 37°C and 5% CO_2 in a humidified incubator. Human iPSC 201B7 cells (Riken BioResource Research Center, Tsukuba, Japan) and patient-derived

iPSCs were routinely maintained in StemFit medium (Ajinomoto Co., Inc., Tokyo, Japan) on cell culture plates coated with iMatrix-511 (0.5 μg/cm^2; Nippi, Incorporated, Tokyo, Japan) [6]. All iPSCs were dissociated into a single-cell suspension using Accutase (Innovative Cell Technologies, Inc., San Diego, CA, USA) and were passaged every 7 days. The Rho-associated coiled-coil-forming kinase (ROCK) inhibitor, Y-27632 (FUJIFILM Wako Pure Chemical Corporation, Osaka, Japan) was added to the medium at 10 μM only on day 1 after passaging. 293T cells (Riken BioResource Research Center) were cultured in Dulbecco's modified Eagle's medium, supplemented with a final concentration of 10% fetal bovine serum (FBS) (JRH Biosciences, Lenexa, KS, USA), and 1% Penicillin/Streptomycin solution (FUJIFILM Wako Pure Chemical Corporation).

Generation of iPSCs from peripheral blood mononuclear cells

Peripheral blood mononuclear cells (PBMCs; 1×10^6) were isolated from peripheral blood of the patient using Ficoll-Paque density gradient medium (GE Healthcare, Chicago, Illinois, USA). The CytoTune-iPS 2.0 Sendai Reprogramming kit (ID Pharma Co., Ltd., Ibaraki, Japan) was used to reprogram the PBMCs, following the

manufacturer's instructions (Fig. S1a). After 14-21 days of transduction, colonies with iPSC morphology were identified under the stereomicroscope and transferred to an iMatrix-511-coated plate filled with StemFit medium.

PCR analyses

All polymerase chain reaction (PCR) analyses were performed using KOD-Plus-Neo polymerase (Toyobo Co., Ltd., Osaka, Japan). The primer sequences and PCR conditions are presented in Table S1.

RNA analyses

Using TRIzol reagent (Invitrogen Corp., Carlsbad, CA, USA), total RNA was isolated from cultured cells. DNA removal and reverse transcription (RT) were performed using ReverTra Ace qPCR RT Master Mix with gDNA Remover (Toyobo Co., Ltd.). RT-PCR analysis of pluripotency marker genes in iPSCs was performed.

To analyze the relative expression of hepatocyte-specific genes in iPSC-derived HLCs, a SYBR green-based quantitative real-time PCR (qPCR) assay was performed in triplicate using the StepOnePlus Real-Time PCR System (Applied Biosystems, Carlsbad, CA, USA). The qPCR conditions are presented in Tables S1 and S2. Relative

expression levels were calculated using the ΔΔCt quantification method. The expression level of each gene was normalized to that of β-2-Microglobulin (*B2M*) as an internal standard. Human fetal liver total RNA (Cell Applications, Inc, San Diego, CA, USA) and human liver total RNA (Agilent Technologies, Inc., Santa Clara, CA, USA) were used as positive controls.

Vector construction

To cleave the intron14 in *F5* by the human codon-optimized *Streptococcus pyogenes* Cas9 (SpCas9) expression vector and single-guide RNA (sgRNA) expression vectors were constructed. Synthetic oligonucleotides with 20-nucleotide guide sequences were ligated into sgRNA expression vectors. The targeting vector was designed with homology arms against *F5* (1.0 kbp in length) containing the corrected sequence. The fluorescent protein monomeric Kusabira-Orange (mKO) fused to a 2A self-cleaving peptide, and the puromycin-N-acetyltransferase cassette, driven by CAG promoter, was then used as the positive selection marker flanked by two different mutant loxP sites (lox66 and lox71).

The LEFiG lentiviral vector containing the polypurine tract (cPPT) of human

immunodeficiency virus-1, the human EF1α promoter, the internal ribosomal entry site (IRES) of the encephalomyocarditis virus, and the enhanced green fluorescent protein (EGFP) was constructed using the pLenti4/TO/V5-DEST (Invitrogen) lentiviral vector backbone. Each cDNA associated with HLC differentiation was inserted into the cloning site of the LEFiG vector.

CRISPR/Cas9-mediated Homology-directed repair (HDR) and excision of the selection cassette by Cre recombinase

Using the Neon electroporation device (Invitrogen Corp.), Cas9 ribonucleoprotein (RNP) complex and targeting vector were transfected into iPSCs. sgRNA was generated using GeneArt Precision gRNA Synthesis kit (Invitrogen Corp.). To establish Cas9 RNP complexes, 1 μg of Alt-R S.p. Cas9 nuclease (Integrated DNA Technologies Inc., San Diego, CA, USA) was added to 10 μL of Resuspension Buffer R (Invitrogen Corp.), followed by 0.2 μg of sgRNA and the mixture was incubated at room temperature for 10 min [7,8]. RNP complexes and 0.8 μg of targeting vector were electroporated into 1×10^5 cells of iPSCs (1200 V, 20 ms, 2 pulses). After 3 days of electroporation, iPSCs were maintained in 0.5 μg/mL of puromycin (Sigma Aldrich, St

Louis, MO, USA) for 7 days. To excise the loxP-floxed selectable marker from knock-in clones, 1 μg of a plasmid expressing Cre recombinase (Addgene plasmid #12106) was electroporated into targeted iPSCs.

Southern blot analysis

BamHI-HF (New England Biolabs Inc., Ipswich, Massachusetts, USA) -digested genomic DNA (10 μg) was electrophoresed in a 1.0% agarose gel and transferred to a Hybond N+ (Amersham Biosciences UK Ltd., Little Chalfont, UK) membrane. Transferred DNA was fixed to the membrane by a UV transilluminator DNA-FIX (ATTO Corporation, Tokyo, Japan). The DNA probe was labeled, hybridized, and detected in accordance with the manufacturer's instructions (AlkPhos Direct Labelling Reagents; Amersham Biosciences UK Ltd.). Hybridized signals were analyzed using an LAS-4000 mini luminescent image analyzer (Fuji Photo Film Co., Ltd., Tokyo, Japan).

***In vitro* hepatic differentiation**

iPSCs were differentiated into HLCs using the Cellartis iPS Cell to Hepatocyte Differentiation System, following the manufacturer's instructions (Takara Bio Europe AB, Gothenburg, Sweden) (Fig. 3A). At the induction of definitive endoderm (DE)

differentiation, iPSCs were seeded in the coated 6-well plate at a density of 4.0 × 10^5/well, and seven days after the start of DE differentiation, the cells were seeded in the coated 24-well plate at a density of 2.0 × 10^5/well. To facilitate endoderm induction and hepatic maturation, several hepatic transcription factors were overexpressed using a lentiviral vector [9]. Briefly, iPSCs were transduced forkhead box transcription factor A2 (FOXA2) on day 2, hepatocyte nuclear factor 1 alpha (HNF1A) on day 5 [10], CCAAT/enhancer-binding protein alpha (C/EBPα) on day 8, activating transcription factor 5 (ATF5) and Prospero homeobox protein 1 (PROX1) on day13 [11]. At the phase of hepatic maturation, the culture supernatants of HLCs were collected when the medium was changed every other day between day 23 and day 34. A total of 30 ml of HLCs culture supernatants was concentrated 200-fold using Vivaspin 20, 100K MWCO ultrafiltration unit (GE Healthcare).

Lentiviral particle production

Lentiviral particles were produced in 293T cells using the ViraPower Lentiviral Expression System (Invitrogen Corp.). After 48h of transfection, virus-containing media

were collected. Multiplicity of infection (MOI) of the lentiviral particles was determined by the number of infected 293T cells.

Immunoassays

For immunostaining of alkaline phosphatase, the Red-Color AP staining kit (System Biosciences, Mountain View, CA, USA) was used. To stain albumin, Goat polyclonal anti-Human Albumin cross-adsorbed Antibody Affinity Purified (A80-229A; Bethyl Laboratories, Inc., Montgomery, TX, USA) and Alexa Fluor 488 donkey anti-goat IgG (H+L) (A-11055; Molecular Probes, Eugene, OR, USA) were used.

The AssayMax Human Factor V ELISA kit (Assaypro LLC, St. Charles, MO, USA) was used to detect FV antigen in the concentrated cell culture supernatant by enzyme-linked immunosorbent assay (ELISA). The standard curve for each quantitative experiment is shown in Figure S4.

FV clotting activity assay

Standard human plasma (Coagtrol N; Sysmex Corporation, Kobe, Japan) and Factor V-deficient plasma (Sysmex Corporation) were used to generate a standard curve for

clotting time of the samples. The FV clotting activity in the concentrated cell culture supernatant was measured based on the PT.

Results

Generation and characterization of iPSCs from patient-derived PBMCs

Patient-derived iPSCs showed normal growth rate and typical human embryonic stem cell (ESC)-like morphology. Several pluripotent stem cell markers, such as alkaline phosphatase activity (Fig. S1b), and mRNA expression of Oct4, SOX2, MYC, KLF4, NANOG, GDF3, REX1, and DMNT3 (Fig. S1c) suggested that established cells were iPSCs.

Gene correction in iPSCs derived from a patient with FV deficiency

The patient had a homozygous point mutation in F5 gene, c.4937C>G (referred to NM_000130.4), resulting in amino acid substitution at p.P1646R. To correct the mutation of *F5* by CRISPR/Cas9-mediated HDR, electroporation was performed using the patient-derived iPSCs. After electroporation and subsequent puromycin selection, mKO-positive iPSC colonies were manually picked and targeted knock-in was verified.

Using the genomic DNA isolated from knock-in clones, the successful gene repair was confirmed by PCR and sequencing (Fig. 2A). Southern blot analysis performed to detect the random integration events revealed that one of the knock-in clones had correct integration (Fig. 2B). PCR conducted to check whether the knock-in was mono- or biallelic confirmed that only monoallelic mutation of *F5* was edited in the knock-in clone (Fig. 2C). Through the screening steps applied to approximately 100 clones, we obtained a single clone with firmly corrected *F5*.

To investigate the off-target mutations due to CRISPR/Cas9 in the gene-corrected iPSCs, sequence analysis was conducted to check for incorrect editing of the sequences similar to the protospacer sequence. Off-target candidate sites were obtained from CRISPR Design (http://crispr.mit.edu/). Off-target mutations were not identified in at least the top 10 candidate sites of off-target editing (Fig. S3).

After the screening for corrected clone, the Cre recombinase expression plasmid was transfected into targeted iPSCs to excise the selection cassette flanked by two loxP sites. After excision of the selection cassettes, the mKO-negative, correct sequence iPSC clone was used for subsequent experiments (Fig. 2C).

Hepatic differentiation of gene-corrected iPSCs

To produce FV, iPSCs were differentiated into HLCs. Human iPSC 201B7 cells were used as a normal control having normal *F5* in both alleles (F5 [wt/wt]). Patient-derived (F5 [mut/mut]) and gene-corrected (F5 [wt/mut]) iPSCs were differentiated into HLCs and the cells revealed typical hepatocyte morphology and were positive for albumin by immunofluorescence staining (Fig. 3B). The mRNA expressions of liver-specific genes such as *AFP* and *ALB* in each HLC were induced to significantly higher levels than those in F5 (wt/wt), F5 (mut/mut) or F5 (wt/mut) iPSCs, and were nearly equivalent to that of positive control. The *F5* mRNA level in F5 (mut/mut) HLCs was 56.0 ± 7.4 times higher compared with that in F5 (mut/mut) iPSCs, and was nearly equivalent to that in F5 (wt/mut) HLCs and F5 (wt/wt) HLCs (Fig. 3C).

The lox72 site still remained at intron 14 of *F5* after the excision of the selection cassette in F5 (mut/mut) iPSCs (Fig. 1). To confirm that the remaining lox72 site did not interfere with the transcription of *F5*, *F5* cDNA was sequenced (Fig. 2D). The cDNA sequence of F5 (wt/mut) HLCs indicated that mRNA was firmly spliced between exon 14 and exon 15, and both the repaired and unrepaired sequences had the same sequence

pattern as the reference (NM_000130.4).

FV antigen and activity levels in the concentrated culture supernatants

A preliminary experiment showed that the amount of FV antigen secreted in the medium was not sufficient to quantify (data not shown), and therefore 200-fold concentrated culture supernatants were used for measurement. F5 (wt/wt) HLCs as normal control showed the FV antigen and specific activity were 101.3 ± 34.2 ng/ml and 210.4 ± 53.2 U/mg, respectively in their culture supernatants. On the other hand, those of F5 (mut/mut) HLCs were not detected (n.d.). In F5 (wt/mut) HLC derived from gene-corrected iPSCs, both the FV antigen and specific activity recovered to 67.0 ± 13.1 ng/ml and 173.2 ± 41.1 U/mg, respectively (Table 1).

Discussion

Over the years, clinical studies of hepatic *in vivo* gene transfer using adeno-associated viral (AAV) vectors for patients with Haemophilia A (HA) and Haemophilia B (HB) have resulted in promising outcomes [12], however there are still concerns regarding immune responses against the AAV vector and inhibitor formation. AAV vectors

exceeding packaging cassettes in excess of 5 kb result in a considerable reduction in viral production yields or transgene recombination. Since the coding sequence length of *F5* is 6.6 kb, incorporating *F5* into the AAV vector is difficult [13]. One of the methods to solve this problem is non-viral gene therapy, particularly gene therapy that includes the application of genome editing. FV deficiency is a monogenic inherited coagulation disorder that is considered to be an ideal indication for gene therapy. Our research has shown the possibility of therapeutic application of genome editing in iPSCs derived from FV-deficient patients.

In this study, we successfully screened a genome-edited clone using the puromycin/mKO selection cassette in obtaining gene repair clones. Some biallelic repaired clones were expected, but we were only able to obtain one monoallelic repaired clone. One of the reasons we could not obtain sufficient number of knock-in clones might be because the targeting vector was too large (10 kb, including 3.8 kb selection cassette), which may have caused low introducing efficiency against iPSCs. As a solution, reducing the size of the targeting vector may improve the efficiency of obtaining editing clones. Other approaches to improve the efficiency of genome editing

may be applicable, such as editing with single-stranded DNA oligonucleotides (ssODN) as a template without selection cassette [14-16]. The reason we did not choose this method was that it would have been necessary to cleave the vicinity of the mutation introduction site, but it was not possible to design a gRNA having specificity for the site. Recently, the novel method called "prime editing" was reported that provides a versatile and precise genome editing without double-strand breaks or donor-DNA, this technology might help our research [17].

Using CRISPR/Cas9-mediated genome editing, only monoallelic mutation of *F5* was corrected in the F5 (mut/mut) iPSCs. If gene repair is successful and differentiated into HLCs, F5 (mut/mut) HLCs should reproduce the patient's pathological condition in which FV antigen and activity are not detected, and the recovery of FV antigen and activity should be observed in F5 (wt/mut) HLCs. As expected, the FV antigen and specific activity in concentrated cell culture supernatants of F5 (wt/mut) HLCs were measured, whereas those of F5 (mut/mut) HLCs were not detected. FV antigen and specific activity in F5 (wt/mut) HLCs were restored at nearly equivalent levels to those in F5 (wt/wt) HLCs.

Considering the mutation of *F5* in this patient, there were few FV antigens in plasma, and a previous report indicated that FV protein was weakly detected in platelet lysate [5], but *F5* mRNA expression level in F5 (mut/mut) HLCs was similar to that of positive control in this study (Fig. 3c). Although the precise mechanism of the effect of this mutation was unclear, it was presumed that the effects occurred after transcriptional stage, such as in translation, processing, or secretion.

There is no curative treatment for FV deficiency, and the available replacement therapy relies only on the administration of fresh-frozen plasma (FFP) [18]. Several approaches for FV deficiency have been considered. Chediak J et al. reported that a patient with acquired FV deficiency unresponsive to FFP was successfully treated with platelet transfusion [19], and C. Bulato et al. reported the development of plasma-derived FV concentration for clinical application and improvement of the clotting activity *in vitro* [20].

Our study shed new light on the gene therapy for FV deficiency, although we did not prove the effectiveness of the gene therapy *in vivo*. A number of supportive studies on the application of iPS-HLCs to cell-based therapy are in progress [21]. Nagamoto et al.

reported that transplantation of an iPSC-derived hepatocyte sheet to the liver surface of a mouse model of acute liver injury ameliorated the fatal liver injury [22]. Okamoto et al. reported that transplantation of iPS-HLCs into the kidney capsule of mice resulted in the generation of functional hepatocyte-like tissue [23]. The transplantations of functional iPS-HLCs into humans have a promising potential for the treatment of FV deficiency.

In summary, we demonstrated that iPSCs could be generated from a patient with FV deficiency and the mutation of *F5* was repaired by CRISPR/Cas9-mediated HDR. Furthermore, we reproduced the patient's pathological condition by differentiation of patient-derived iPSCs into HLCs and succeeded in recovering clotting activity of FV with gene-corrected HLCs. To our knowledge, this is the first report of gene repair of iPSCs derived from a patient with FV deficiency. Gene-edited iPSCs will hold promise for gene therapy of inherited coagulation disorders as a potential cell source for autologous cell transplantation.

Addendum

T. Nakamura contributed to all experiments in the collection and interpretation of the data, and wrote the manuscript. S. Morishige performed experiments and analyzed data. H. Ozawa performed experiments and analyzed and interpreted the data. K. Kuboyama performed experiments and analyzed data. T. Okamura supervised experiments. S. Mizuno contributed to the study concept and the study design and supervised research. K. Nagafuji critically revised the manuscript. All authors discussed the results and approved the final version of the manuscript.

Disclosure of Conflict of Interests

The authors state that they have no conflict of interest.

Supporting Information

Additional supporting information may be found online in the Supporting Information section at the end of the article.

Fig. S1. Generation and characterization of iPSCs from patient-derived PBMCs

Fig. S2. Genome editing efficiency in 293T cells

Fig. S3. CRISPR/Cas9-mediated off-target mutations analysis

Fig. S4. Standard curves for FV antigen level and clotting activity

Table S1. Primer sets and PCR conditions used in this study

Table S2. Primers for qPCR analysis

References

1. Asselta R, Peyvandi F. Factor V deficiency. *Seminars in thrombosis and hemostasis.* 2009;35(4):382-389.
2. Mali P, Yang L, Esvelt KM, et al. RNA-guided human genome engineering via Cas9. *Science (New York, NY).* 2013;339(6121):823-826.
3. Cong L, Ran FA, Cox D, et al. Multiplex genome engineering using CRISPR/Cas systems. *Science (New York, NY).* 2013;339(6121):819-823.
4. Jinek M, Chylinski K, Fonfara I, Hauer M, Doudna JA, Charpentier E. A programmable dual-RNA-guided DNA endonuclease in adaptive bacterial immunity. *Science (New York, NY).* 2012;337(6096):816-821.
5. Kanaji S, Kanaji T, Honda M, et al. Identification of four novel mutations in F5 associated with congenital factor V deficiency. *International journal of hematology.* 2009;89(1):71-75.
6. Nakagawa M, Taniguchi Y, Senda S, et al. A novel efficient feeder-free culture system for the derivation of human induced pluripotent stem cells. *Sci Rep.* 2014;4:3594.
7. Liang X, Potter J, Kumar S, et al. Rapid and highly efficient mammalian cell engineering via Cas9 protein transfection. *Journal of biotechnology.* 2015;208:44-53.
8. Kim S, Kim D, Cho SW, Kim J, Kim JS. Highly efficient RNA-guided genome editing in human cells via delivery of purified Cas9 ribonucleoproteins. *Genome research.* 2014;24(6):1012-1019.
9. Morishige S, Mizuno S, Ozawa H, et al. CRISPR/Cas9-mediated gene correction in hemophilia B patient-derived iPSCs. *International journal of hematology.* 2019.
10. Takayama K, Inamura M, Kawabata K, et al. Generation of metabolically functioning hepatocytes from human pluripotent stem cells by FOXA2 and HNF1alpha transduction. *Journal of hepatology.* 2012;57(3):628-636.
11. Nakamori D, Takayama K, Nagamoto Y, et al. Hepatic maturation of human iPS cell-derived hepatocyte-like cells by ATF5, c/EBPalpha, and PROX1 transduction. *Biochem Biophys Res Commun.* 2016;469(3):424-429.
12. Perrin GQ, Herzog RW, Markusic DM. Update on clinical gene therapy for hemophilia. *Blood.* 2019;133(5):407-414.

13. Naso MF, Tomkowicz B, Perry WL, 3rd, Strohl WR. Adeno-Associated Virus (AAV) as a Vector for Gene Therapy. *BioDrugs : clinical immunotherapeutics, biopharmaceuticals and gene therapy.* 2017;31(4):317-334.
14. Ran FA, Hsu PD, Wright J, Agarwala V, Scott DA, Zhang F. Genome engineering using the CRISPR-Cas9 system. *Nat Protoc.* 2013;8(11):2281-2308.
15. Yang L, Guell M, Byrne S, et al. Optimization of scarless human stem cell genome editing. *Nucleic acids research.* 2013;41(19):9049-9061.
16. Salsman J, Dellaire G. Precision genome editing in the CRISPR era. *Biochemistry and cell biology = Biochimie et biologie cellulaire.* 2017;95(2):187-201.
17. Anzalone AV, Randolph PB, Davis JR, et al. Search-and-replace genome editing without double-strand breaks or donor DNA. *Nature.* 2019.
18. Menegatti M, Peyvandi F. Treatment of rare factor deficiencies other than hemophilia. *Blood.* 2019;133(5):415-424.
19. Chediak J, Ashenhurst JB, Garlick I, Desser RK. Successful management of bleeding in a patient with factor V inhibitor by platelet transfusions. *Blood.* 1980;56(5):835-841.
20. Bulato C, Novembrino C, Anzoletti MB, et al. "In vitro" correction of the severe factor V deficiency-related coagulopathy by a novel plasma-derived factor V concentrate. *Haemophilia : the official journal of the World Federation of Hemophilia.* 2018;24(4):648-656.
21. Tolosa L, Pareja E, Gomez-Lechon MJ. Clinical Application of Pluripotent Stem Cells: An Alternative Cell-Based Therapy for Treating Liver Diseases? *Transplantation.* 2016;100(12):2548-2557.
22. Nagamoto Y, Takayama K, Ohashi K, et al. Transplantation of a human iPSC-derived hepatocyte sheet increases survival in mice with acute liver failure. *Journal of hepatology.* 2016;64(5):1068-1075.
23. Okamoto R, Takayama K, Akita N, et al. Human iPS Cell-based Liver-like Tissue Engineering at Extrahepatic Sites in Mice as a New Cell Therapy for Hemophilia B. *Cell transplantation.* 2018;27(2):299-309.
24. Schneider CA, Rasband WS, Eliceiri KW. NIH Image to ImageJ: 25 years of image analysis. *Nature methods.* 2012;9(7):671-675.

25. Hsu PD, Scott DA, Weinstein JA, et al. DNA targeting specificity of RNA-guided Cas9 nucleases. *Nature biotechnology.* 2013;31(9):827-832.

26. Bishi DK, Mathapati S, Venugopal JR, et al. Trans-differentiation of human mesenchymal stem cells generates functional hepatospheres on poly(l-lactic acid)-co-poly(ε-caprolactone)/collagen nanofibrous scaffolds. *Journal of Materials Chemistry B.* 2013;1(32).

27. Vossaert L, O'Leary T, Van Neste C, et al. Reference loci for RT-qPCR analysis of differentiating human embryonic stem cells. *BMC molecular biology.* 2013;14:21.

Figure legends

Fig. 1. Schematic representation of the HDR-mediated gene correction strategy for the mutant allele in *F5*

Point mutation existed in exon 14 of the *F5* genome of patient-derived iPSCs. Targeting construct had homology arms that contained exon 14 of *F5* with correct sequence, and the selection cassette existed between the two homology arms. Cas9/gRNA ribonucleoprotein (RNP) complexes made a double-strand DNA breaks (DSB) in intron14 of *F5* (scissors). After the HDR-mediated knock-in of the targeting construct into the genomic locus, mKO-positive and puromycin-resistant clones were screened. The successful knock-in clones were identified by PCR and sequencing. The selection cassette flanked by two mutant loxP sites (lox66 and lox71) was removed by transient transduction of Cre recombinase expression plasmid.

Fig. 2. Gene correction in iPSCs derived from a patient with FV deficiency

(A) *Sequence analysis of edited allele*

DNA sequencing of patient-derived iPSCs showed homozygous missense mutation of C>G in exon14 of *F5*, whereas that of edited allele in knock-in iPSC clones revealed the correction of the causing mutation, using primers that detect only the edited genome.

(B) *Southern blot analysis of knock-in clones*

The size of expected DNA fragments was 2709 bp (black arrowheads). Genomic DNA derived from a non-transfected iPSC clone was used as the negative control (NC) (1). A candidate clone (2) had correct integration. Brightness and contrast were adjusted.

(C) *Sequence of loxP sites in knock-in clone after Cre-mediated excision*

The electropherogram showed the genomic DNA sequence around of lox72 site of *F5* (wt/mut) iPSC after the transfection of Cre recombinase expression vector, indicating the cassette flanked by two loxP sites was firmly excised.

(D) *cDNA sequence of gene-corrected iPSC-derived hepatocytes*

The cDNA sequence of gene-corrected iPSC-derived HLCs showed that the transcription product contained both the corrected and uncorrected sequences. While exogenous lox72 site remained in intron 14 of gene-corrected *F5* genome, mRNA was firmly spliced between exon 14 and exon 15.

Fig. 3. *In vitro* hepatic differentiation

(A) *Schematic representation of the HLCs differentiation protocol*

iPSCs were differentiated into HLCs *in vivo* using the Cellartis iPS Cell to Hepatocyte Differentiation System. To facilitate endoderm induction and hepatic maturation, iPSCs were transduced FOXA2 on day 2, HNF1A on day 5, C/EBPα on day 8, ATF5 and PROX1 on day13 using a lentiviral vector.

(B) *Images of HLCs differentiated from iPSCs and albumin immunofluorescence staining*

Bright-field cell image of HLCs after 23 days of culture (a and b, 100x magnification). Albumin immunofluorescence staining of HLCs after 23 days of culture (c and d, 100x magnification). a and c: F5 (mut/mut) HLCs, b and d: F5 (wt/mut) HLCs

F5 (mut/mut): patient-derived, F5 (wt/mut): gene-corrected

(C) *Relative quantification of hepatocyte-related genes and F5 mRNA*

The hepatocyte-specific genes and *F5* mRNA expression fold changes of iPSCs or HLCs relative to the levels in F5 (mut/mut) iPSCs were calculated. The hepatocyte-specific genes and *F5* mRNA expression were measured using StepOnePlus. Relative

expression levels were calculated using the ΔΔCt quantification method, and each signal was normalized with the value of β-2-Microglobulin (*B2M*). The data are presented as the mean fold change of expression levels of each cell type with respect to those of F5 (mut/mut) iPSCs.

F5 (wt/wt): normal control

Fig. 1.

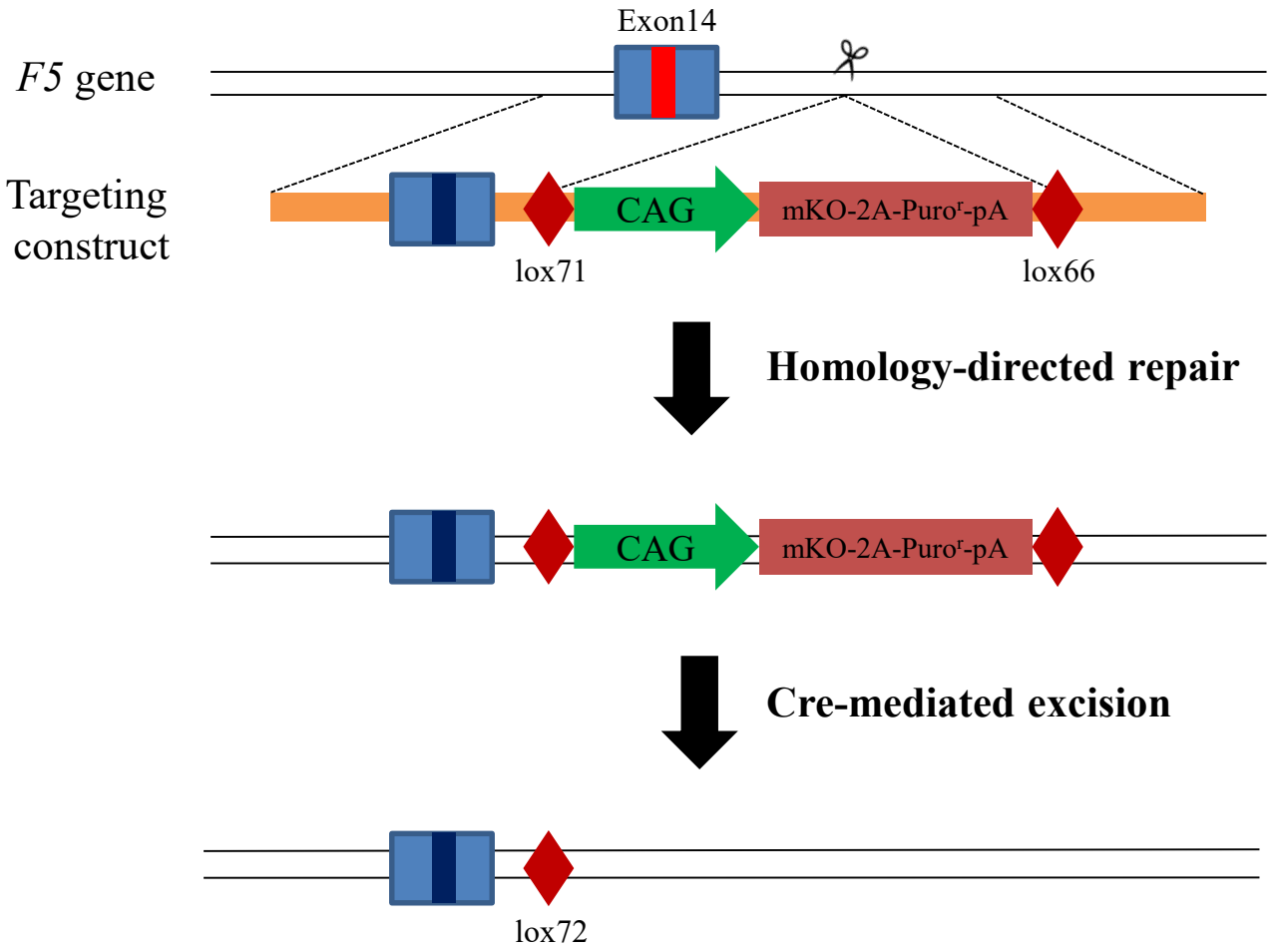
Exon14
F5 gene
Targeting construct
CAG
mKO-2A-Puro^r-pA
lox71
lox66
Homology-directed repair
CAG
mKO-2A-Puro^r-pA
Cre-mediated excision
lox72

Fig. 2. (A)

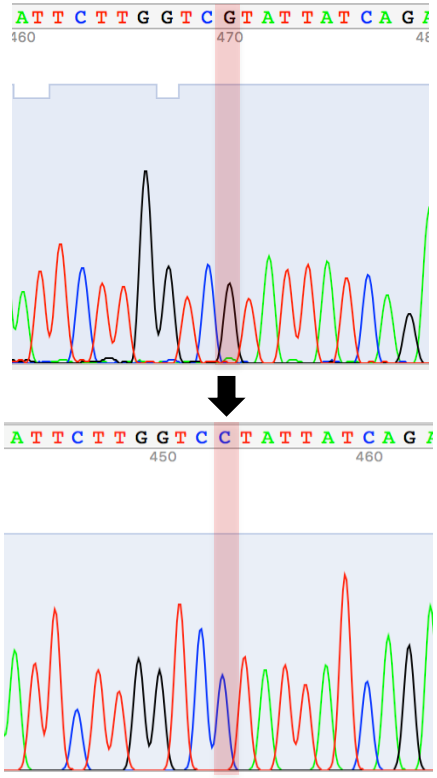

(B)

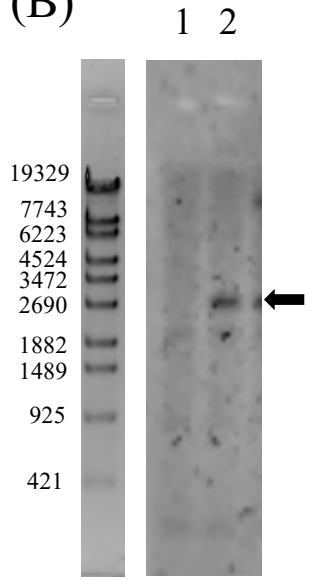

(C)

Left arm lox72 Right arm

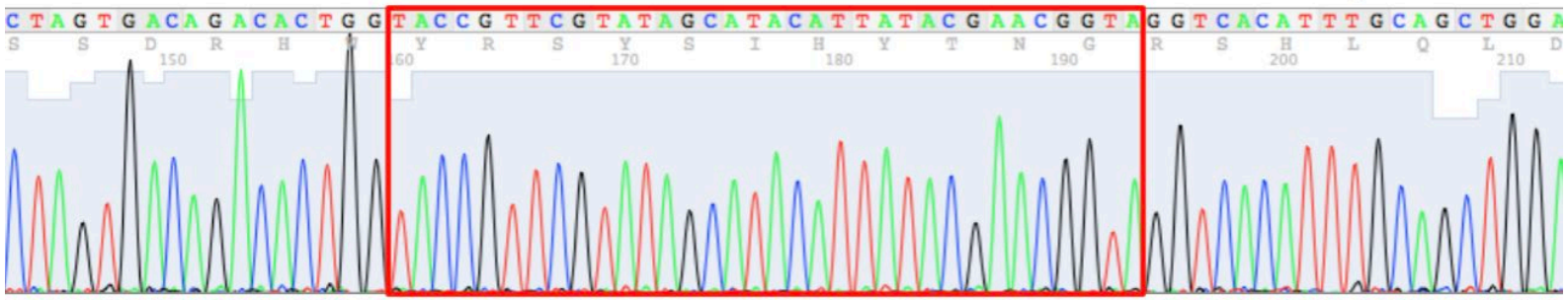

(D)

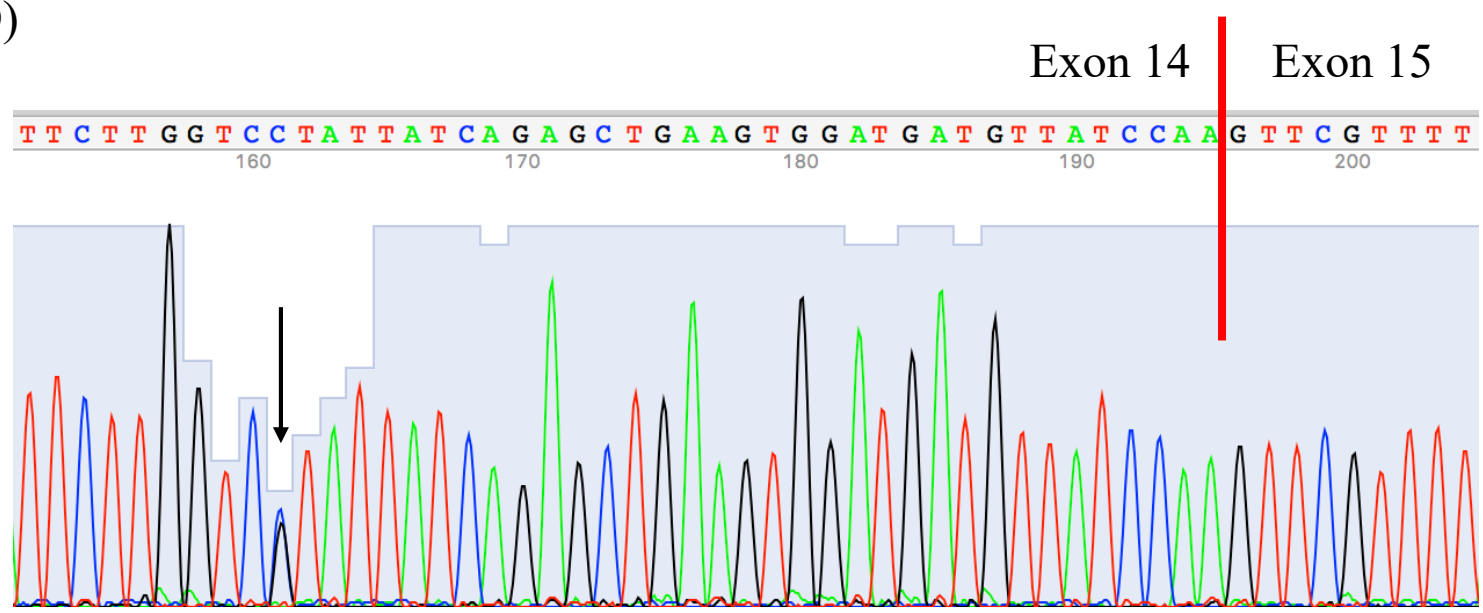
Exon 14
Exon 15
T T C T T G G T C C T A T T A T C A G A G C T G A A G T G G A T G A T G T T A T C C A A G T T C G T T T T
160
170
180
190
200

Figure 3.

(A)

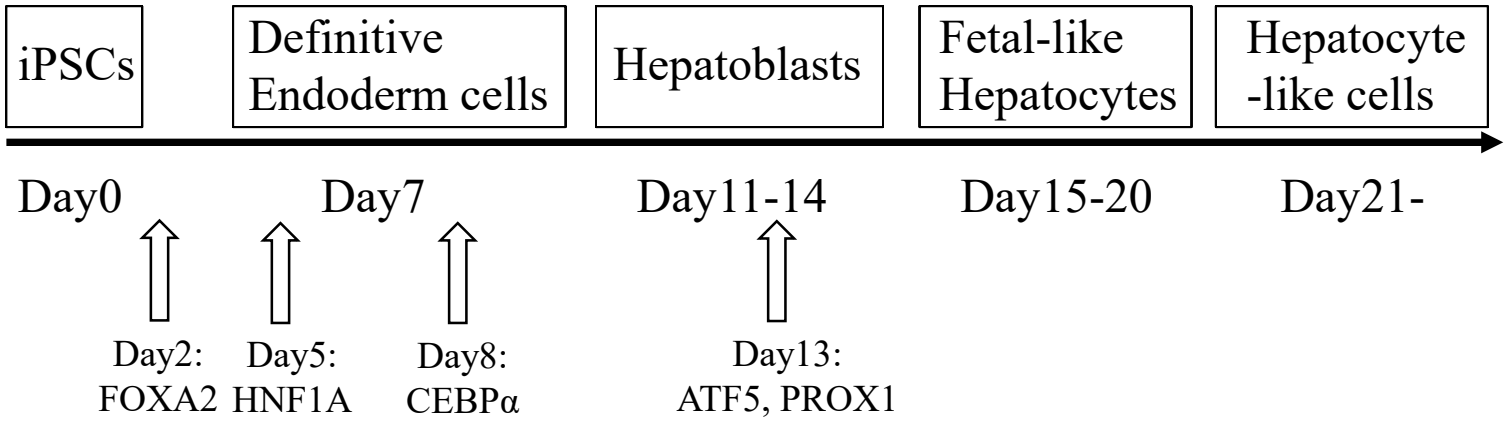
iPSCs
Definitive Endoderm cells
Hepatoblasts
Fetal-like Hepatocytes
Hepatocyte -like cells
Day0
Day7
Day11-14
Day15-20
Day21-
Day2: FOXA2
Day5: HNF1A
Day8: CEBPα
Day13: ATF5, PROX1

(B)

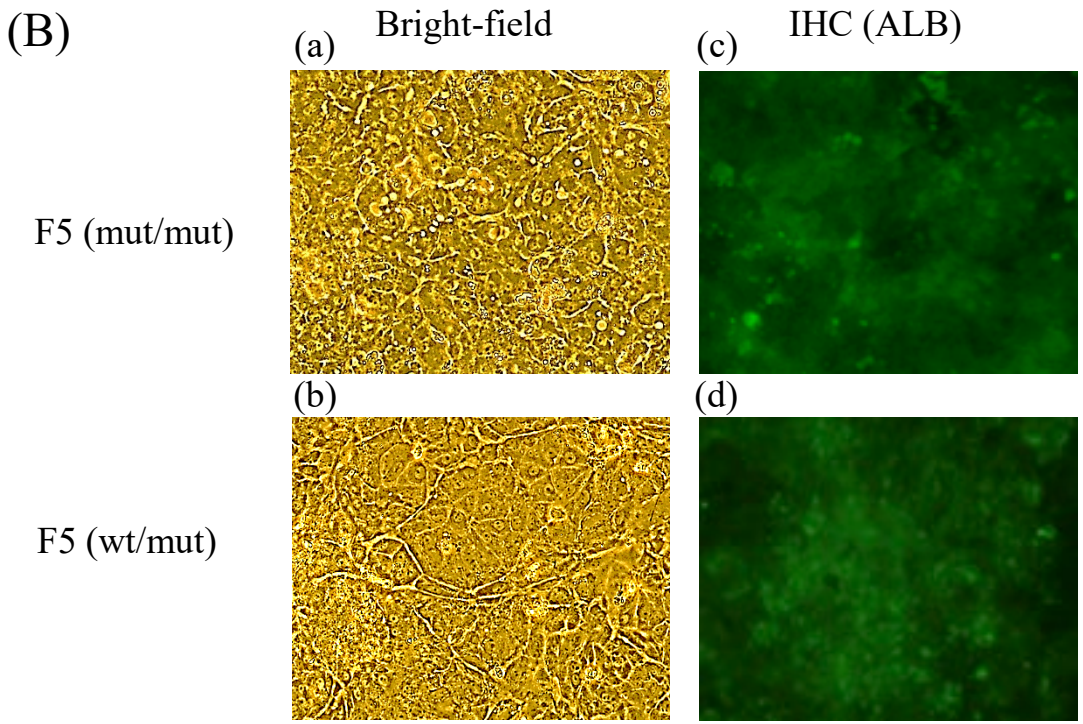
Bright-field
IHC (ALB)
(a)
(c)
F5 (mut/mut)
(b)
(d)
F5 (wt/mut)

(C)

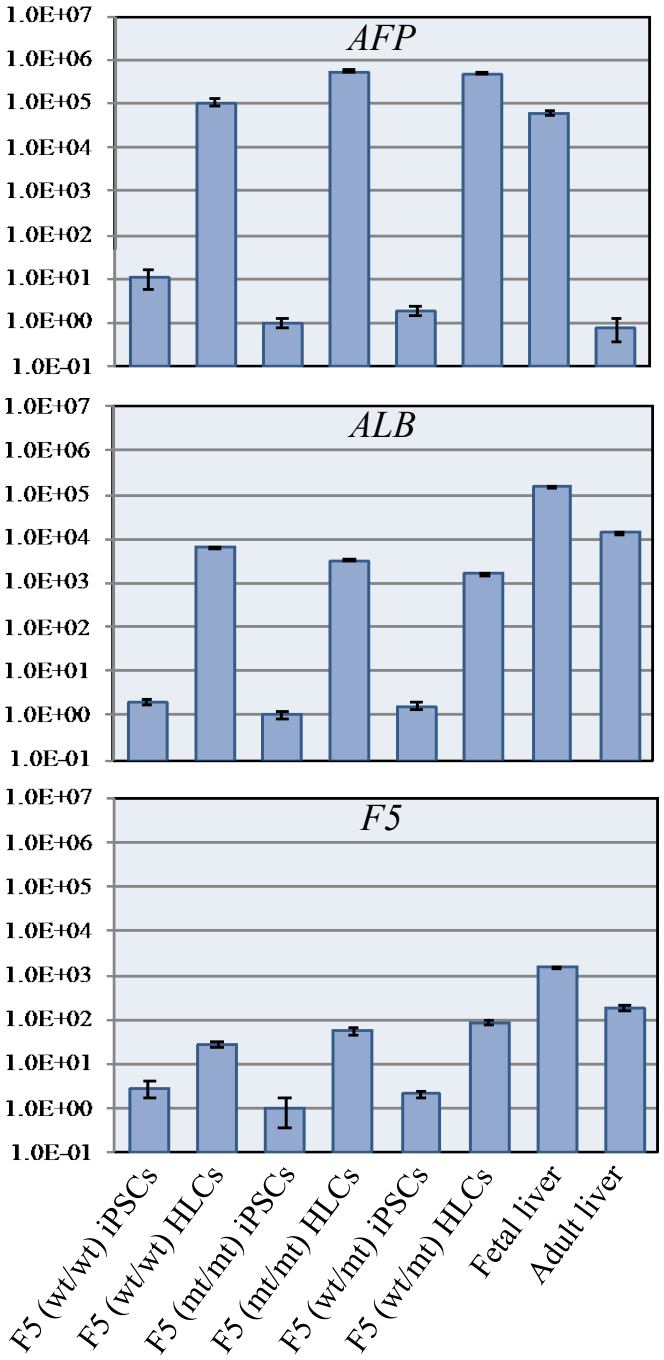
AFP
ALB
F5
1.0E+07
1.0E+06
1.0E+05
1.0E+04
1.0E+03
1.0E+02
1.0E+01
1.0E+00
1.0E-01
F5 (wt/wt) iPSCs
F5 (wt/wt) HLCs
F5 (mt/mt) iPSCs
F5 (mt/mt) HLCs
F5 (wt/mt) iPSCs
F5 (wt/mt) HLCs
Fetal liver
Adult liver

Table 1. FV antigen levels and clotting activities in the culture supernatants

	FV antigen (ng/mL)	final volume after concentration (µl)	total FV antigen in supernatants (ng)	FV clotting activity of supernatants* （%)	FV clotting activity of standard plasma** （%)	FV specific activity（U/mg)
F5 (wt/wt) HLCs	101.3 ± 34.2	163.3 ± 18.9	16.3 ± 4.8	2.1 ± 0.5	1.5 ± 0.5	210.4 ± 53.2
F5 (mut/mut) HLCs	n.d.	153.3 ± 4.7	n.d.	n.d.	n.d.	n.d.
F5 (wt/mut) HLCs	67.0 ± 13.1	183.3 ± 33.0	12.1 ± 2.1	1.2 ± 0.4	1.0 ± 0.2	173.2 ± 41.1

F5 (wt/wt): normal control, F5 (mut/mut): patient-derived, F5 (wt/mut): gene-corrected

Values indicate mean ± SD.

Unit definition: One unit is equivalent to the Factor V activity in 1ml of normal human plasma.

FV specific activity of standard plasma: 142.9 U/mg

Each experiment was performed in triplicate.

*5µl of the supernatants were used for activity measurement.

**Clotting activities of standard plasma correspond to the same amount of FV antigen in culture supertants.

Fig. S1.

a)

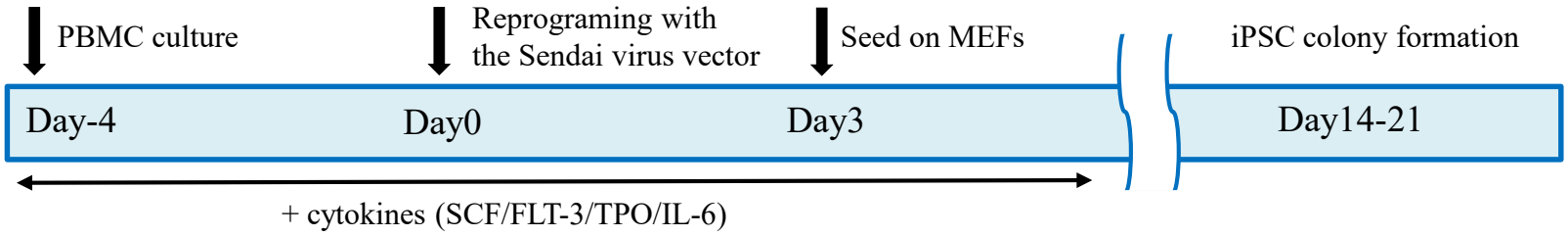
PBMC culture
Reprograming with
the Sendai virus vector
Seed on MEFs
iPSC colony formation
Day-4
Day0
Day3
Day14-21
+ cytokines (SCF/FLT-3/TPO/IL-6)

b)

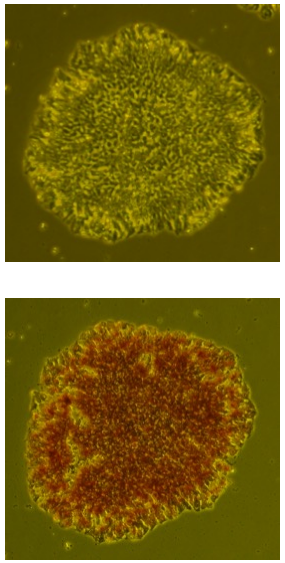

c)

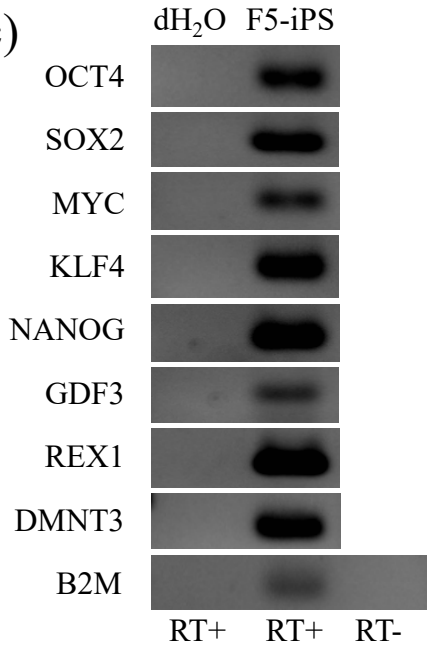
dH2O
F5-iPS
OCT4
SOX2
MYC
KLF4
NANOG
GDF3
REX1
DMNT3
B2M
RT+
RT+
RT-

Fig. S1.

Generation and characterization of iPSCs from patient-derived PBMCs

a) **Schematic representation of the generation of iPSCs from PBMCs using Sendai virus**
PBMCs were isolated from peripheral venous blood of the patient using Ficoll-Paque density gradient medium. Reprogramming of the PBMCs was conducted using the Sendai virus vector containing reprogramming factors.

b) **Images of patient-derived iPSCs and alkaline phosphatase immunofluorescence staining**
Bright-field cell image of an iPSC colony after 21 days of reprogramming (200x magnification, upper figure).
Alkaline phosphatase staining (200x magnification, lower figure).
iPSC lines showed alkaline phosphatase activity.

c) **RT-PCR analysis of pluripotent marker genes in iPSCs**
RT-PCR analysis of pluripotency marker genes in iPSCs was performed. Each experiment was conducted in triplicate, and the PCR products were analyzed on 2% agarose gels. dH2O instead of F5-iPS cDNA was used as a negative control. The absence of genomic DNA was confirmed by B2M PCR with F5-iPS mRNA without RT.

Fig. S2.

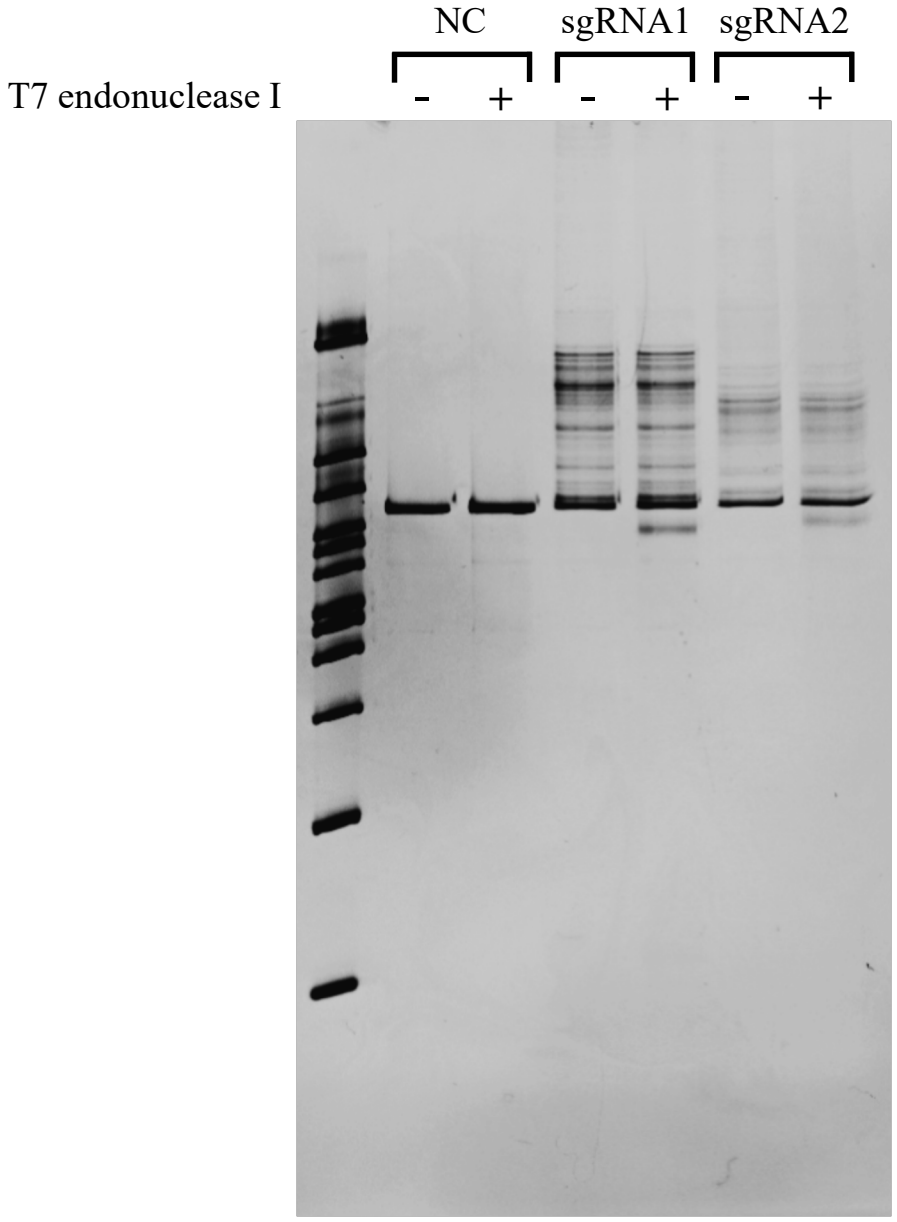

Fig. S2.

Genome editing efficiency in 293T cells

The expression vector for each sgRNA was constructed to verify the digestion activity in the presence of SpCas9. Two guide sequences (sgRNA1:GTTACAACCCTCTGGTGCTTG, sgRNA2: GTGAGATCCCACTCAAGGCC) were designed from the intron 14 region of *F5*. To evaluate the cleavage efficiency, 293T cells were co-transfected with each sgRNA expression vector and a plasmid vector encoding SpCas9. Using T7 endonuclease I (T7E1) assay, insertion/deletion (Indel) events in 293T cells were detected. PCR amplification products (400 ng) in NEBuffer2 (NEB) were denatured and reannealed to produce heteroduplex, and the reannealed PCR products were treated with 4 units of T7E1 (NEB) at 37˚C for 15 min. The products were loaded on 12.5% polyacrylamide gels. The relative intensity of the DNA bands was quantified using ImageJ software [24]. As a negative control, the reannealed PCR products without treatment of T7E1 were loaded on polyacrylamide gels. The indel percentage was calculated using the following formula: indel (%) = 100 x [1 − (1 − sum of intensities of the cleaved products/(sum of intensities of the undigested PCR product and the cleaved products))$^{1/2}$] [25]. To perform CRISPR/Cas9-mediated HDR in iPSCs, we selected the most efficient sgRNA (sgRNA 1), containing a targeting sequence located 84 bp downstream from the mutation site.

Fig. S3.

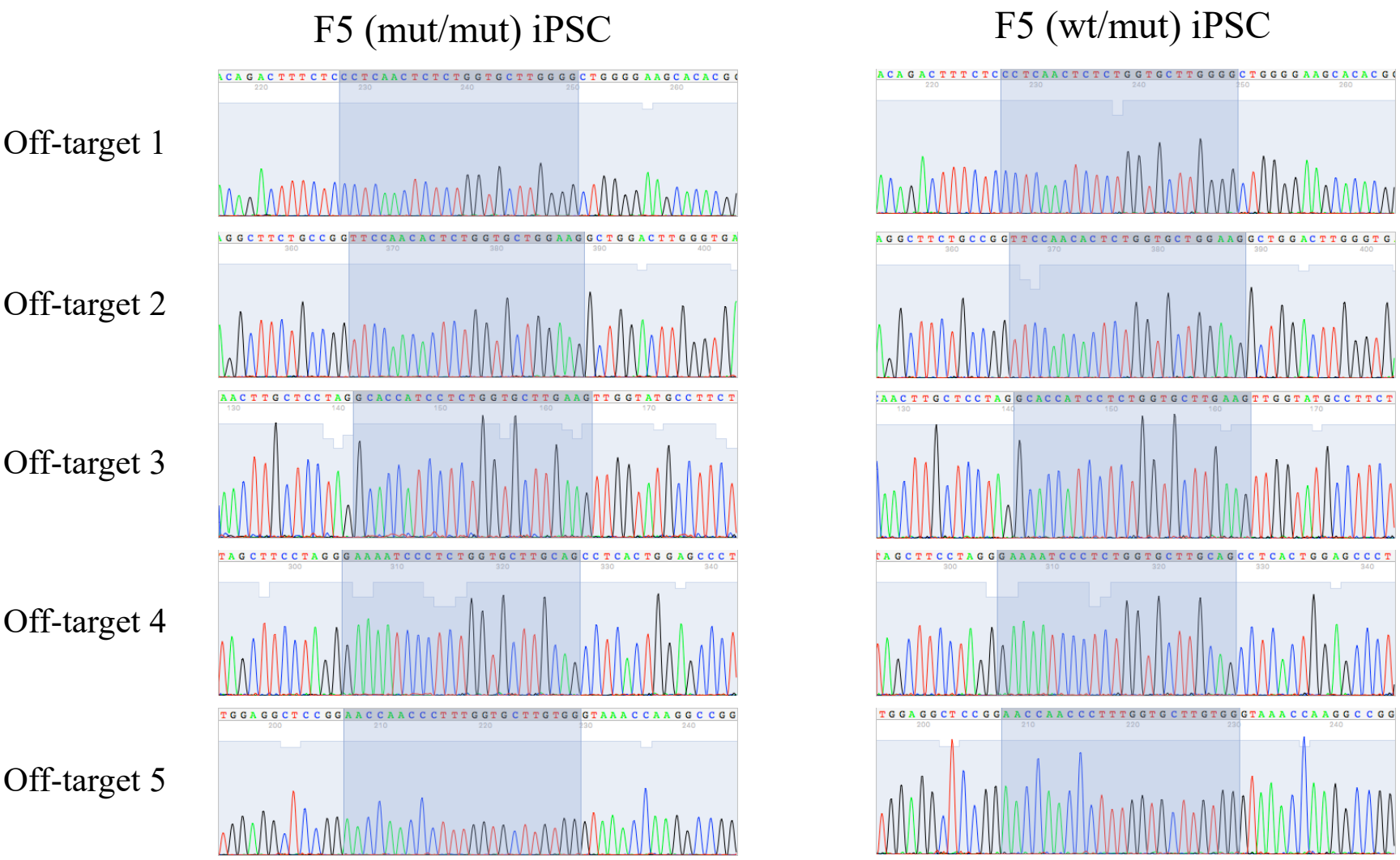
F5 (mut/mut) iPSC
F5 (wt/mut) iPSC
Off-target 1
Off-target 2
Off-target 3
Off-target 4
Off-target 5

	F5 (mut/mut) iPSC	F5 (wt/mut) iPSC
Off-target 6	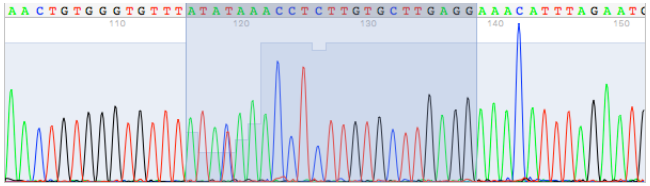	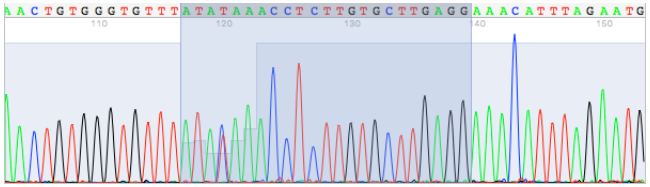
Off-target 7	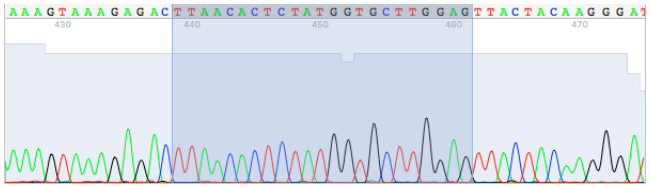	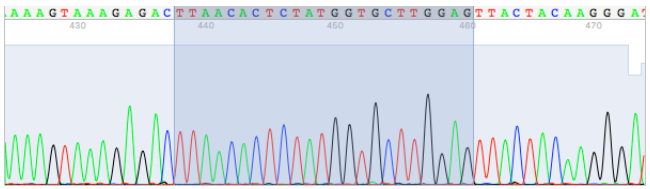
Off-target 8	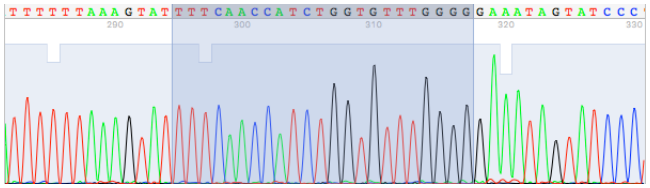	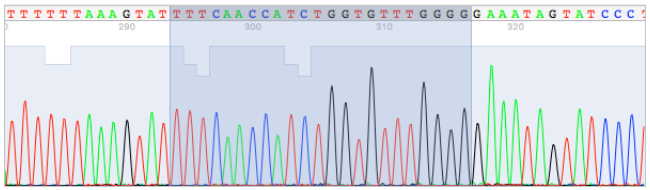
Off-target 9	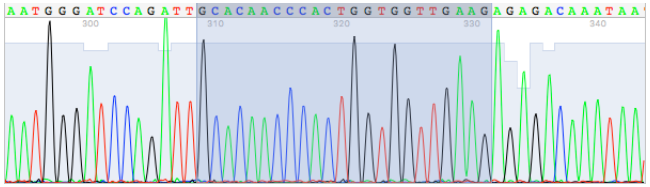	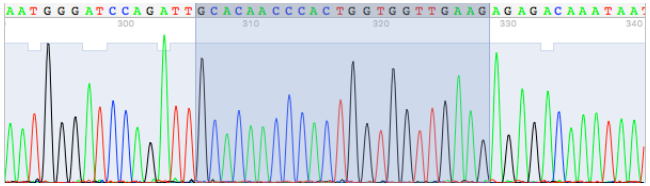
Off-target 10	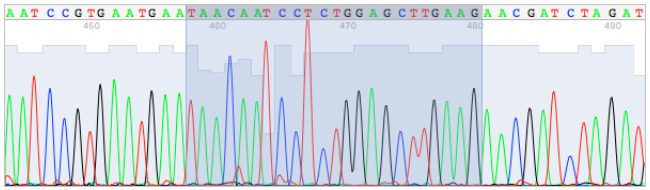	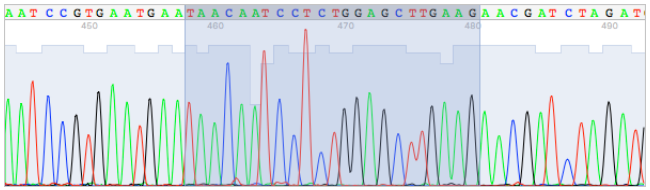

Fig. S3.

CRISPR/Cas9-mediated off-target mutations analysis

To investigate the off-target mutations in F5 (wt/mut) iPSCs, the sequences similar to the sgRNA sequence were confirmed by sequence analysis. Off-target candidate sites were obtained from CRISPR Design (http://crispr.mit.edu/). The top ten off-target candidate sites were PCR amplified, and the PCR products were then subjected to sequence analyses. This analysis showed that the sequence of at least the top ten off-target candidate sites did not change after editing. Off-target mutations due to CRISPR/Cas9 were not detected in this analysis.

Fig. S4.

a)

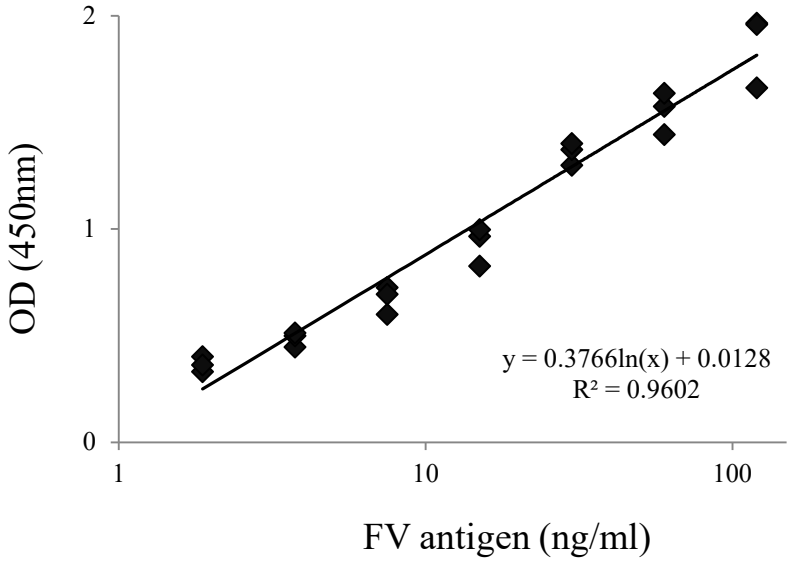
OD (450nm)
2
1
0
1
10
100
y = 0.3766ln(x) + 0.0128
R² = 0.9602
FV antigen (ng/ml)

b)

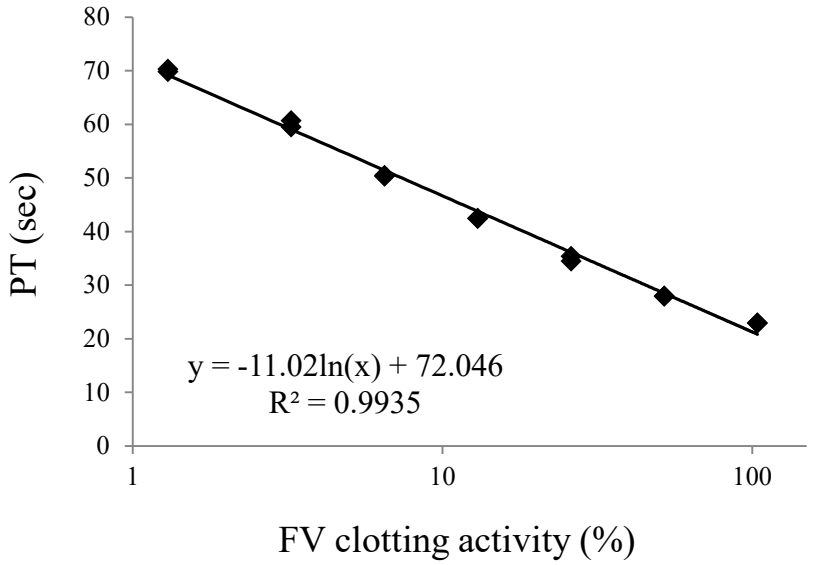
PT (sec)
80
70
60
50
40
30
20
10
0
1
10
100
y = -11.02ln(x) + 72.046
R² = 0.9935
FV clotting activity (%)

Fig. S4.

Standard curves for FV antigen level and clotting activity

a) Standard curve for FV antigen level (ELISA)

Standard FV antigen included in the ELISA kit was used to generate a standard curve for FV antigen level. The approximation was performed by the least-squares method. Experiment for preparing the standard curve were performed in triplicate.

b) Standard curve for FV clotting activity

Standard human plasma and Factor V-deficient plasma were used to generate a standard curve for clotting time of the samples. The approximation was performed by the least-squares method. Experiment for preparing the standard curve were performed in duplicate.

Table S1. Primer sets and PCR conditions used in this study.

Primer name	Primer sequence	Product size (bp)	Applications	Conditions
F5Left-F	ATTGTCACCTGATAGCCCCAAGC	826	PCR for generating left homology arms	Stepdown
F5Left-R	AAATTCCTCCGAAGATCTTAGCAGTGC			
F5Right-L	CCACAAGCACCAGAGGGTTGTAA	734	PCR for generating right homology arms	Stepdown
F5Right-R	TGCCTCCCATAGCTTCATGGAAAA			
CelI-F	AGCAAACTAGGCACAATGGCTGA	759	PCR for T7E1 assay	Stepdown
CelI-R	ATTGCTTGGCAAGGAGTCTTTGAA			
F5-HR5-F1	ACCCATCCAGTGACTTTCATAAGTGTG	1294	PCR for detecting the 5′-junction site, sequencing	Stepdown
F5-HR5-R1	GGAAAGTCCCATAAGGTCATGTACTGG			
F5-HR3-F1	GAGGTCATCAGTATATGAAACAGCCCC	1066	PCR for detecting the 3′-junction site	Stepdown
F5-HR3-R1	TCGTTCATCTTGAAAAAGGATCCCCTA			
hOCT3/4-S1165	GACAGGGGGAGGGGAGGAGCTAGG	144	Endo OCT3/4 RT-PCR	RT-PCR (excluding KLF4)
hOCT3/4-AS1283	CTTCCCTCCAACCAGTTGCCCCAAAC			
hSOX2-S1430	GGGAAATGGGAGGGGTGCAAAAGAGG	151	Endo SOX2 RT-PCR	RT-PCR (excluding KLF4)
hSOX2-AS1555	TTGCGTGAGTGTGGATGGGATTGGTG			
hREX1-RT-U	CAGATCCTAAACAGCTCGCAGAAT	306	Rex1 RT-PCR	RT-PCR (excluding KLF4)
hREX1-RT-L	GCGTACGCAAATTAAAGTCCAGA			
hDNMT3B-S2502	TGCTGCTCACAGGGCCCGATACTT C	242	DNMT3B RT-PCR	RT-PCR (excluding KLF4)
hDNMT3B-S2716	TCCTTTCGAGCTCAGTGCACCACAAAAC			
NANOG-F	TGAACCTCAGCTACAAACAG	154	NANOG RT-PCR	RT-PCR (excluding KLF4)
NANOG-R	TGGTGGTAGGAAGAGTAAAG			
MYC-F	ACTCTGAGGAGGAACAAGAA	159	MYC RT-PCR	RT-PCR (excluding KLF4)
MYC-R	TGGAGACGTGGCACCTCTT			
GDF3-F	AAATGTTTGTGTTGCGGTCA	179	GDF3 RT-PCR	RT-PCR (excluding KLF4)
GDF3-R	TCTGGCACAGGTGTCTTCAG			
KLF4q2-F	ATTACCAAGAGCTCATGCCACC	220	KLF4 RT-PCR	RT-PCR (KLF4)
KLF4q2-R	AATTTCCATCCACAGCCGTC			
B2MqF2	TGCTGTCTCCATGTTTGATGTATCT	86	B2M RT-PCR	RT-PCR (excluding KLF4)
B2MqR2	TCTCTGCTCCCCACCTCTAAGT			
F5RT-1F	TGATTATGTGCCCTATGATGACCCCTA	504	F5 RT-qPCR	cDNA sequence
F5RT-1R	ACGTAGGTATAACTGCTATTTGGCTGA			
F5LoxPCR-F	AAGTACCTCGACAGCACTTTTACCAAA	298	PCR for screening of Cre-loxP-mediated excision	Stepdown
F5LoxPCR-R	ATTGCTTGGCAAGGAGTCTTTGAA			
F5offF1-1	ACCTCAGTTGAGGGCTGACTGTA	410	F5 off target 1	3step
F5offR1-1	CCACGTCAAGATGGAGGCAGAAA			
F5offF2-1	GCCCATGAAAGGCAGAACTGAGA	669	F5 off target 2	3step
F5offR2-1	ATGTTTACCAAAGCCCTCCCACC			
F5offF3-1	TGGTCCCCCTGGTTCTCTTACTC	675	F5 off target 3	3step
F5offR3-1	ATTGTCCTAGGAGGCTTTTGGGC			
F5offF4-1	CCCAGTGAACACGAGTGCCATTA	518	F5 off target 4	3step
F5offR4-1	5-TTTGGAAGCAGTGGGTGAGATGG			
F5offF5-1	AATTCCTGGTAAAGGGCCCGAAC	424	F5 off target 5	3step
F5offR5-1	GCTGGGCTGTTCCTTAACCACAT			
F5offF6-1	TGCTAGCAGATCCACCAGTGTCT	396	F5 off target 6	3step
F5offR6-1	ACAGGCTGTCATTCCTGTGCATT			
F5offF7-1	ATTCTAGCAGTGTTCTGCCTGCC	573	F5 off target 7	3step
F5offR7-1	GCATCTGTAAGGAACCAGGCCAA			
F5offF8-1	GCGCAAAGCAGTAAAGAAAGGGG	436	F5 off target 8	3step
F5offR8-1	TGACACTCATGGTCCTATCAAGAAACA			
F5offF9-1	AGAGATGAACCCAGGGTAGCACA	512	F5 off target 9	3step
F5offR9-1	AGGGAGATGAAGAGCAGTGGTGA			
F5offF10-1	GCAGAGGCTAACACCACCAATCA	563	F5 off target 10	3step
F5offR10-1	CCATGACTTTAGCGCAGGGGAAT			

PCR conditions

Stepdown	94°C 2 m, [98°C 10 s, 74°C 30 s] x5, [98°C 10 s, 72°C 30 s] x5, [98°C 10 s, 70°C 30 s] x5, [98°C 10 s, 68°C 30 s] x22, 68°C 5 m, 4°C
RT-PCR (excluding KLF4)	94°C 2 m, [98°C 10 s, 58°C 30 s, 68°C 30 s] x40
RT-PCR (KLF4)	94°C 2 m, [98°C 10 s, 63°C 20 s, 68°C 20 s] x40
cDNA sequence	94°C 2 m, [98°C 15 s, 63°C 15 s, 68°C 30 s] x35, 68°C 5 m, 4°C
3step	94°C 2 m, [98°C 10 s, 63°C 30 s, 68°C 30 s] x35, 68°C 3 m, 4°C

Table S2. Primers for qPCR analysis

Primers for SYBR Green-based qPCR	Primer sequence
AFP -F	ACAGCAGCCACTTGTTGCCA
AFP -R	TGGCCAACACCAGGGTTTAC
ALB -F	TAAGGAGACCTGCTTTGCCG
ALB -R	AGACAGGGTGTTGGCTTTACA
F5 -F	GGCAGCAGACATCGAACAGC
F5 -R	ATGCTCTCAGGCACATAGCCA
GAPDH -F	TGCACCACCAACTGCTTAGC
GAPDH -R	GGCATGGACTGTGGTCATGAG
B2M -F	TGCTGTCTCCATGTTTGATGTATCT
B2M -R	TCTCTGCTCCCCACCTCTAAGT

qPCR program: 95°C 1 m, [95°C 5 s, 60°C 30 s] x42

Reference

HNF4A,AFP : [26]
B2M : [27]